# Density Functional Studies on 19-Electron Metal Sandwich Complexes: Electronic Structures of $CpFe(\eta^6\text{-}C_6H_6)$, $CpFe(\eta^6\text{-}C_6Me_6)$, and $(C_5Me_5)Fe(\eta^6\text{-}C_6H_6)$

Dale A. Braden and David R. Tyler*

*Department of Chemistry, University of Oregon, Eugene, Oregon 97403-1253*

*Received January 18, 2000*

Density functional theory (DFT) calculations were carried out on three 19-electron metal sandwich complexes, $CpFe(\eta^6\text{-}C_6H_6)$, $CpFe(\eta^6\text{-}C_6Me_6)$, and $(C_5Me_5)Fe(\eta^6\text{-}C_6H_6)$, to determine their electronic structure. The nuclear quadrupole splittings for these three molecules were also calculated using DFT and were found to be in reasonable agreement with the experimental values observed by Mössbauer spectroscopy. For $CpFe(\eta^6\text{-}C_6H_6)$ and $(C_5Me_5)Fe(\eta^6\text{-}C_6H_6)$, the metal contributions to the singly occupied molecular orbital (SOMO) were found to be about 45% and 30%, respectively, lower than estimates based on the magnitude of the quadrupole splitting. In the case of $CpFe(\eta^6\text{-}C_6Me_6)$, however, the SOMO is dominated by the permethylated arene ligand, while the metal contribution is only about 10%, much less than the estimate of 75% based on the quadrupole splitting. In all three molecules the spin density is concentrated around the iron atom, and the partial charge on the iron atom is 0.75, as calculated using the AIM method. It is concluded that the determination of the composition of a molecular orbital based on comparing the observed quadrupole splitting for a molecule to the estimated splitting for the free atom is too approximate to be reliable and that consideration of a single molecular orbital does not allow a reliable estimate of the net charge or spin density around an atom in a molecule.

Downloaded by CARLI CONSORTIUM on June 29, 2009
Published on February 24, 2000 on http://pubs.acs.org | doi: 10.1021/om000034f

## Introduction

In 1979−1981, Astruc et al. described a series of 19-electron metal sandwich complexes[1−4] based on $CpFe(\eta^6\text{-}C_6H_6)$,[5,6] a compound which had been previously synthesized by Nesmeyanov et al.[7,8] but not isolated. Astruc's group characterized these complexes by EPR, UV−vis, Mössbauer, and cyclic voltammetry, and one of them, $CpFe(\eta^6\text{-}C_6Me_6)$, was stable enough to be crystallized and characterized by X-ray diffraction. Estimates of the unpaired electron occupation of the iron valence orbitals based on the Mössbauer data and on extended Hückel or Xα calculations yielded a wide range of values from 53 to 83% for some of these molecules.[1,5,6,9−11] Although these were approximate calculations, they did suggest high localization of the unpaired electron on the metal atom in these complexes. This contrasts with what we have found using density functional theory (DFT) for 19-electron adducts such as $CpCo(CO)_2^-$ and $Mn(CO)_5Cl^-$, where the metal population was 20−30%.[12,13] To see how the electronic structure of the 19-electron metallocenes compares to that of the 19-electron adducts, we performed DFT calculations on three metallocenes: $CpFe(\eta^6\text{-}C_6H_6)$, $CpFe(\eta^6\text{-}C_6Me_6)$, and $(C_5Me_5)Fe(\eta^6\text{-}C_6H_6)$.

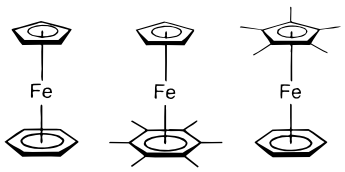


These molecules were chosen because they are among the very few 19-electron metal sandwich complexes for which experimental data are available. Computationally modeling this series of molecules also allows us to explore the effect of permethylation on each of the ligands relative to the unsubstituted molecule. Density functional theory was used as the computational method because it has been successful in reproducing experimentally measured nuclear quadrupole couplings for iron[14−18] and other elements.[19,20] It has also been used

(1) Astruc, D. *Chem. Rev.* **1988**, *88*, 1189−1216.
(2) Tyler, D. R. *Acc. Chem. Res.* **1991**, *24*, 325−331.
(3) Tyler, D. R. In *Organometallic Radical Processes*; Trogler, W. C., Ed.; Elsevier: New York, 1990; pp 338−364.
(4) Geiger, W. E. *Acc. Chem. Res.* **1995**, *28*, 351−357.
(5) Hamon, J.-R.; Astruc, D.; Michaud, P. *J. Am. Chem. Soc.* **1981**, *103*, 758−766.
(6) Astruc, D.; Hamon, J.-R.; Althoff, G.; Román, E.; Batail, P.; Michaud, P.; Mariot, J.-P.; Varret, F.; Cozak, D. *J. Am. Chem. Soc.* **1979**, *101*, 5445−5447.
(7) Nesmeyanov, A. N.; Vol'kenau, N. A.; Bolesova, I. N. *Dokl. Akad. Nauk SSSR* **1966**, *166*, 607.
(8) Nesmeyanov, A. N.; Vol'kenau, N. A.; Sirotkina, E. I.; Deryabin, V. V. *Dokl. Akad. Nauk SSSR* **1967**, *177*, 1110.
(9) Le Beuze, A.; Lissillour, R.; Weber, J. *Organometallics* **1993**, *12*, 47−55.
(10) Lacoste, M.; Rabaa, H.; Astruc, D.; Le Beuze, A.; Saillard, J.-Y.; Précigoux, G.; Courseille, C.; Ardoin, N.; Bowyer, W. *Organometallics* **1989**, *8*, 2233−2242.
(11) Mariot, J. P.; Michaud, P.; Lauer, S.; Astruc, D.; Trautwein, A. X.; Varret, F. *J. Phys. (Les Ulis, Fr.)* **1983**, *44*, 1377−1385.
(12) Braden, D. A.; Tyler, D. R. *Organometallics* **1998**, *17*, 4060−4064.
(13) Braden, D. A.; Tyler, D. R. *J. Am. Chem. Soc.* **1998**, *120*, 942−947.
(14) Godbout, N.; Havlin, R.; Salzmann, R.; Debrunner, P. G.; Oldfield, E. *J. Phys. Chem. A* **1998**, *102*, 2342−2350.

10.1021/om000034f CCC: $19.00 © 2000 American Chemical Society
Publication on Web 02/24/2000

to model the 17- and 18-electron analogues of CpFe($\eta^6$-$C_6H_6$) and related complexes.[21]

## Computational Methods

All calculations were performed using Gaussian 98.[22] The geometries of all three molecules were optimized using the BP86, B3P86, and B3LYP density functionals in a spin-unrestricted formalism.[23] The BP86 and B3P86 functionals were included because DFT calculations on a variety of metallocenes containing a first-row transition metal have indicated that they yield more accurate geometries for these kinds of molecules than the more popular B3LYP functional.[24] Wave function stability calculations were run on all wave functions to ensure that they did not correspond to excited states, at least with respect to single excitations.

The TZV basis set of Ahlrichs et al. was used for all atoms.[25,26] The basis included one d polarization function on carbon and one f function and two p functions on iron. The exponents of the p functions were equal to those of the two most diffuse s functions, and the exponent for the f function was 2.462.[27] The quadrupole splitting (mm/s) for the iron atom in each geometry-optimized complex was calculated according to eq 1, where $e$ is the electronic charge, $c$ is the speed of light,

$$\mathrm{QS} = \frac{1000 ecQV_{zz}}{8\pi\epsilon_0 a_0^3 E_\gamma}\left(1 + \frac{\eta^2}{3}\right)^{1/2} \qquad (1)$$

$Q$ is the quadrupole moment of iron (in $m^2$), $V_{zz}$ is the largest eigenvalue of the electric field gradient tensor (typically given in atomic units, $\mathrm{bohr}^{-3}$), $\epsilon_0$ is the vacuum permittivity, $a_0$ is the bohr radius, $E_\gamma$ is the energy of the $\gamma$-radiation used in the Mössbauer experiment (14 413 eV),[28] and $\eta$ is the asymmetry parameter, which is defined as $(V_{xx} - V_{yy})/V_{zz}$. The electric field gradient is the quantity calculated using DFT. To calculate the quadrupole splitting, the quadrupole moment, $Q$, of the nucleus of interest must be known. For $^{57}$Fe, this quantity has been the subject of numerous investigations. The two most recent computational studies arrived at values of 0.11[29] and 0.16 barn,[30] respectively, while the most recent spectroscopic study yielded a value of 0.11−0.12 barn.[31] A reviewer recommends the value of 0.15 ± 0.02 barn for covering the range of reliable values.[32] We have chosen the latter number on the basis of this recommendation and because its associated error range can be propagated into the calculated quadrupole splittings (see Table 2).

There are two possible relative orientations of the rings in the three molecules examined here that preserve a mirror plane of symmetry:

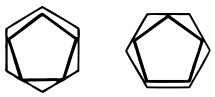

The crystal structure of CpFe($\eta^6$-$C_6Me_6$) has the second of these two conformations,[6] and this is the geometry chosen for all three molecules in the optimizations. The energy difference between these two conformations is small, and the alternative structure was not expected to give significantly different results for the calculated properties. DFT calculations on both conformations of CpFe($\eta^6$-$C_6H_6$)$^+$ showed that the barrier to interconversion was only 0.002 eV.[21] Furthermore, the crystal structure of $[(C_5Me_5)Fe(\text{perylene})]^+PF_6^-$ contains both conformations, which suggests that the energy difference between them is small.[10] Finally, our calculations on $CpCo(CO)_2^-$ indicated that the difference in calculated hyperfine coupling constants between the two possible conformations with $C_s$ symmetry was negligible.[13]

## Results and Discussion

**Geometries.** The crystal structure of CpFe($\eta^6$-$C_6Me_6$) shows that both rings are planar and parallel, and essentially untilted (i.e., the dihedral angle between the rings was 0.82°).[6] In fact, the calculated structures for all three molecules show these same characteristics. The deviations of the Cp and benzene rings from planarity are too small to indicate any decrease in hapticity. The C−C bond lengths in the Cp rings differ by 0.04 Å at most (for a given computational method), and the C−C bonds in the benzene rings differ by 0.02 Å at most, which indicates that the ring $\pi$ systems are well delocalized. As we have found for other metallocenes,[24]

Downloaded by CARLI CONSORTIUM on June 29, 2009
Published on February 24, 2000 on http://pubs.acs.org | doi: 10.1021/om000034f

(15) Godbout, N.; Sanders, L. K.; Salzmann, R.; Havlin, R. H.; Wojdelski, M.; Oldfield, E. *J. Am. Chem. Soc.* **1999**, *121*, 3829−3844.
(16) Havlin, R. H.; Godbout, N.; Salzmann, R.; Wojdelski, M.; Arnold, W.; Schulz, C. E.; Oldfield, E. *J. Am. Chem. Soc.* **1998**, *120*, 3144−3151.
(17) McMahon, M. T.; deDios, A. C.; Godbout, N.; Salzmann, R.; Laws, D. D.; Le, H.; Havlin, R. H.; Oldfield, E. *J. Am. Chem. Soc.* **1998**, *120*, 4784−4797.
(18) Salzmann, R.; McMahon, M. T.; Godbout, N.; Sanders, L. K.; Wojdelski, M.; Oldfield, E. *J. Am. Chem. Soc.* **1999**, *121*, 3818−3828.
(19) Salzmann, R.; Kaupp, M.; McMahon, M. T.; Oldfield, E. *J. Am. Chem. Soc.* **1998**, *120*, 4771−4783.
(20) Eriksson, L. A.; Malkina, O. L.; Malkin, V. G.; Salahub, D. R. *Int. J. Quantum Chem.* **1997**, *63*, 575−583.
(21) Ruiz, J.; Ogliaro, F.; Saillard, J.-Y.; Halet, J.-F.; Varret, F.; Astruc, D. *J. Am. Chem. Soc.* **1998**, *120*, 11693−11705.
(22) Frisch, M.; Robb, M.; Cheeseman, J. R.; Stratmann, R.; Burant, J.; Dapprich, S.; Daniels, A.; Kudin, K.; Strain, M.; Farkas, O.; Barone, V.; Cossi, M.; Cammi, R.; Mennucci, B.; Pomelli, C.; Clifford, S.; Ochterski, J.; Petersson, G.; Ayala, P.; Cui, Q.; Morokuma, K.; Malick, D.; Rabuck, A.; Raghavachari, K.; Foresman, J.; Cioslowski, J.; Ortiz, J.; Stefanov, B.; Liu, G.; Liashenko, A.; Piskorz, P.; Komaromi, I.; Gomperts, R.; Martin, R.; Fox, D.; Keith, T.; Al-Laham, M.; Peng, C.; Nanayakkara, A.; Gonzalez, C.; Challacombe, M.; Gill, P. M. W.; Johnson, B.; Chen, W.; Wong, M.; Andres, J.; Gonzalez, C.; Head-Gordon, M.; Replogle, E.; Pople, J. Gaussian 98, Rev. A.6; Gaussian, Inc., Pittsburgh, PA, 1998.
(23) Pople et al. have explained why restricted open-shell DFT has no theoretical basis and why $\langle S^2 \rangle$ for a Kohn−Sham wave function should not be expected to be equal to $S(S + 1)$: Pople, J. A.; Gill, P. M. W.; Handy, N. C. *Int. J. Quantum Chem.* **1995**, *56*, 303. See also: Wang, J.; Becke, A. D.; Smith, V. H., Jr. *J. Chem. Phys.* **1995**, *102*, 3477.
(24) Braden, D. A.; Tyler, D. R. Unpublished work.
(25) Schäfer, A.; Huber, C.; Ahlrichs, R. *J. Chem. Phys.* **1994**, *100*, 5829−5835.
(26) Basis sets were obtained from the Extensible Computational Chemistry Environment Basis Set Database, Version 1.0, as developed and distributed by the Molecular Science Computing Facility, Environmental and Molecular Sciences Laboratory, which is part of the Pacific Northwest Laboratory, P.O. Box 999, Richland, WA 99352, and funded by the U.S. Department of Energy. The Pacific Northwest Laboratory is a multiprogram laboratory operated by Battelle Memorial Institute for the U.S. Department of Energy under Contract DE-AC06-76RLO 1830. Contact David Feller, Karen Schuchardt, or Don Jones for further information.
(27) Ehlers, A. W.; Böhme, M.; Dapprich, S.; Gobbi, A.; Höllwarth, A.; Jonas, V.; Köhler, K. F.; Stegmann, R.; Veldkamp, A.; Frenking, G. *Chem. Phys. Lett.* **1993**, *208*, 111−114.
(28) Firestone, R. B. *Table of Isotopes*, 8th ed.; Wiley: New York, 1998.
(29) Hagelberg, F.; Das, T. P. *Z. Naturforsch., A* **1998**, *53*, 358−361.
(30) Dufek, P.; Blaha, P.; Schwarz, K. *Phys. Rev. Lett.* **1995**, *75*, 3545−3548.
(31) Su, Z.; Coppens, P. *Acta Crystallogr.* **1996**, *A52*, 748−756.
(32) A reviewer pointed out that the calculated value of 0.16 barn for $Q(^{57}Fe)$ was recently revised to 0.17 barn and provided the following reference: Blaha, P. International Conference on the Application of the Mössbauer Effect, 1999. As of the time of this writing, this reference has not been published. The reviewer also pointed out that the spectroscopic determination of 0.11−0.12 barn was based in part on an anomalous data point and that if this data point was removed, the value becomes about 0.13 barn. In the reviewer's opinion, the most reliable value is 0.15 barn, as calculated by: Ray, S. N.; Das, T. P. *Phys. Rev. B* **1977**, *16*, 4794. Lauer, S.; Marathe, V. R.; Trautwein, A. *Phys. Rev. A* **1979**, *19*, 1852. Hence, the reviewer's preference is 0.15 ± 0.02 barn for $Q(^{57}Fe)$.

**Table 1. Experimental and Calculated Geometries for CpFe($\eta^6$-$C_6Me_6$)[a]**

| | exptl | BP86 | B3P86 | B3LYP |
|---|---|---|---|---|
| C−C (Cp) | 1.371(6) | 1.439 | 1.425 | 1.427 |
| | av 1.403(6) | 1.416, 1.448 | 1.405, 1.434 | 1.407, 1.436 |
| C−C (Bz) | 1.293(8) | 1.450 | 1.435 | 1.439 |
| | 1.366(9) | 1.430 | 1.415 | 1.419 |
| | av 1.428(9) | 1.450, 1.429 | 1.434, 1.415 | 1.438, 1.418 |
| RMSD | | 0.063 | 0.053 | 0.055 |
| Fe−C( Cp) | av 2.144(4) | 2.121, 2.198, 2.169 | 2.121, 2.193, 2.165 | 2.163, 2.232, 2.207 |
| Fe−C (Bz) | av 2.100(7) | 2.109, 2.227, 2.110 | 2.103, 2.210, 2.105 | 2.139, 2.247, 2.140 |
| RMSD | | 0.040 | 0.033 | 0.070 |

[a] Where the experimental bond lengths are reported as averaged values, the calculated bond lengths were also weight-averaged before calculating the root mean square deviations (RMSD). Distances are given in Å.

the hybrid density functionals yield shorter CC bond lengths and longer M−C bond lengths compared to "pure" functionals such as BP86, and the LYP correlation functional consistently gives longer bonds than P86.

Only a few of the bond lengths and angles found by X-ray diffraction for CpFe($\eta^6$-$C_6Me_6$) were reported, and some of these were averages. These are collected in Table 1, where they are compared to the DFT results. The experimental bond length of 1.293 Å for one of the delocalized C−C bonds in the benzene ring is as short as that of the fully localized double bond in cyclopropene (1.293 Å),[33] which is one of the shortest known (cf. 1.331 Å for ethylene[34] and 1.311 Å for tetrafluoroethylene[35]). The C−C bonds in dibenzenechromium are 1.42 Å in length.[36] Two other C−C bonds, one in the benzene ring at 1.366 Å and the other in the Cp ring at 1.371 Å, are also surprisingly short. We found that the RMS deviation between calculated and experimental C−C bond lengths for metallocenes ranging from vanadocene to nickelocene was 0.002 Å using the BP86 functional and 0.010 Å using the B3P86 functional.[24] These deviations from experimental geometries are much less than those for CpFe($\eta^6$-$C_6Me_6$) (see Table 1) and give confidence that the geometry for CpFe($\eta^6$-$C_6Me_6$) calculated using either BP86 or B3P86 is acceptable. The crystal structure of CpFe($\eta^6$-$C_6Me_6$) was determined at 293 K,[6] but the Mössbauer experiments showed that a phase transition occurred at about 190 K.[37] This suggests that the molecular geometry at low temperature, which corresponds more closely to the calculated structure, is different from that at room temperature, although the extremely short C−C bond length of 1.293 Å is still suspect.[38]

Permethylation of either ring causes an increase in the C−C bond lengths in that ring. However, permethylation affects the bonding of the rings to the iron atom differently. Permethylation of the benzene ring causes an increase in the Fe−C(benzene) distances (BP86 geometries: 2.134 Å (av) for CpFe($\eta^6$-$C_6H_6$) vs 2.149 Å (av) for CpFe($\eta^6$-$C_6Me_6$)), whereas permethylation of the Cp ring actually causes a slight decrease in Fe−C(Cp) distances (BP86 geometries: 2.179 Å (av) for CpFe($\eta^6$-$C_6H_6$) vs 2.178 Å (av) for ($C_5Me_5$)Fe($\eta^6$-$C_6H_6$)). The latter effect is due to a decrease in the Fe−Cp(centroid) distance, which more than offsets the effect of ring expansion. Thus, permethylation of the Cp ring binds it tighter to the metal. This is consistent with a wealth of experimental observations that compounds containing the pentamethylcyclopentadienide ligand are generally more kinetically stable than those with the unsubstituted Cp ligand.[39,40]

**Mössbauer Parameters.** Table 2 contains the electric field gradients and quadrupole splittings calculated by DFT for CpFe($\eta^6$-$C_6H_6$), CpFe($\eta^6$-$C_6Me_6$), and ($C_5Me_5$)Fe($\eta^6$-$C_6H_6$) compared to the experimental values. Because finite temperature effects are not included in the computational model, the calculated values should be compared to the experimental values obtained at very low temperature. The quadrupole coupling constants and isomer shifts for CpFe($\eta^6$-$C_6H_6$) and CpFe($\eta^6$-$C_6Me_6$) were recorded at a variety of temperatures down to 4.2 K, but those for ($C_5Me_5$)Fe($\eta^6$-$C_6H_6$) were reported only for measurements at 77 K.[5] The Mössbauer parameters for all of the 19-electron CpFe(arene) compounds showed a strong temperature dependence, their magnitudes increasing with decreasing temperature. Thus, the quadrupole coupling and isomer shift for ($C_5Me_5$)Fe($\eta^6$-$C_6H_6$) would be expected to be higher at 4.2 K than at 77 K and comparable to those values for CpFe($\eta^6$-$C_6H_6$) and CpFe($\eta^6$-$C_6Me_6$). The value of the isomer shift for ($C_5Me_5$)Fe($\eta^6$-$C_6H_6$) at 77 K is anomalously low compared to the isomer shifts for CpFe($\eta^6$-$C_6H_6$), CpFe($\eta^6$-$C_6Me_6$), CpFe($\eta^6$-$C_6Et_6$), and ($C_5Me_5$)Fe($\eta^6$-$C_6Me_6$) at the same temperature.[5,41]

Table 2 shows that at 77 K the experimental quadrupole splittings decrease in magnitude in the order CpFe($\eta^6$-$C_6Me_6$) > CpFe($\eta^6$-$C_6H_6$) > ($C_5Me_5$)Fe($\eta^6$-$C_6H_6$). This trend is reproduced by the DFT calculations. Quantitative comparisons between the calculated and experimental values are only possible for CpFe($\eta^6$-$C_6Me_6$) and CpFe($\eta^6$-$C_6H_6$) because only these two compounds were experimentally examined at very low temperature (4.2 K), which is close to the effective temperature of absolute zero in the calculations. The quadrupole splitting calculated using the BP86 density functional agrees very well with the experimental value for CpFe($\eta^6$-$C_6Me_6$) but is high in the case of CpFe($\eta^6$-$C_6H_6$). The quadrupole splittings calculated using the hybrid functionals B3P86 and B3LYP are all too high. The LYP correlation functional gives consistently larger

(33) Berry, R. J.; Harmony, M. D. *Struct. Chem.* **1990**, *1*, 49−59.
(34) Martin, J. M. L.; Taylor, P. R. *Chem. Phys. Lett.* **1996**, *248*, 336−344.
(35) Carlos, J. L., Jr.; Karl, R. R., Jr.; Bauer, S. H. *J. Chem. Soc., Faraday Trans. 2* **1974**, *21*, 177−187.
(36) Keulen, E.; Jellinek, F. *J. Organomet. Chem.* **1966**, *5*, 490−492.
(37) Mariot, J. P.; Guillin, J.; Varret, F.; Lauer, S.; Trautwein, A. *Hyperfine Interact.* **1986**, *30*, 221−251.
(38) Another well-known cause for anomalously short C−C bond lengths in rings is due to an approximation made in the XRD data fitting. For atoms constrained to move along an arc, as in the librational motion of rings, the associated electron density traces out a crescent shape. XRD data analysis programs generally cannot handle this kind of shape and, instead, treat it as an ellipsoid. Because the centroids of the ellipsoids (which are taken to represent the nuclear positions) are closer to the center of the ring than the centroids of the crescents, the ring bond lengths appear to be shorter. This is a possible explanation for the short C−C bond lengths reported for CpFe($\eta^6$-$C_6Me_6$): Weakley, T. J. R. Personal communication. See also: Dunitz, J. D. *X-ray Analysis and the Structure of Organic Molecules*; Cornell University Press: Ithaca, NY, 1979; pp 248−249.
(39) Okuda, J. *Top. Curr. Chem.* **1992**, *160*, 97−145.
(40) Janiak, C. *Adv. Organomet. Chem.* **1991**, *33*, 291−393.
(41) Mariot, J.-P.; Varret, F.; Michaud, P.; Astruc, D.; Hamon, J.-R.; Althoff, G.; Batail, P. *J. Phys., Colloq.* **1980**, *41*, 319−320.

Downloaded by CARLI CONSORTIUM on June 29, 2009
Published on February 24, 2000 on http://pubs.acs.org | doi: 10.1021/om000034f

**Table 2. Calculated EFG Tensor Eigenvalues, $V_{ii}$ (au), Quadrupole Splittings, QS (mm/s), and Isomer Shifts, IS (mm/s), for CpFe($\eta^6$-$C_6H_6$), ($C_5Me_5$)Fe($\eta^6$-$C_6H_6$), and CpFe($\eta^6$-$C_6Me_6$)**

| | CpFe($\eta^6$-$C_6Me_6$) | | | | CpFe($\eta^6$-$C_6H_6$) | | | | ($C_5Me_5$)Fe($\eta^6$-$C_6H_6$) | | | |
|---|---|---|---|---|---|---|---|---|---|---|---|---|
| | exptl[a] | BP86 | B3P86 | B3LYP | exptl[a] | BP86 | B3P86 | B3LYP | exptl[a] | BP86 | B3P86 | B3LYP |
| $V_{xx}$ | | −0.4508 | −0.4825 | −0.4526 | | −0.3956 | −0.5736 | −0.5365 | | −0.3148 | −0.5338 | −0.5390 |
| $V_{yy}$ | | −0.5535 | −0.7948 | −0.9249 | | −0.5689 | −0.6365 | −0.7670 | | −0.5717 | −0.5773 | −0.6595 |
| $V_{zz}$ | | 1.0043 | 1.2773 | 1.3775 | | 0.9645 | 1.2101 | 1.3035 | | 0.8865 | 1.1111 | 1.1984 |
| $\eta$[b] | | 0.10 | 0.24 | 0.34 | | 0.18 | 0.05 | 0.18 | | 0.29 | 0.04 | 0.10 |
| QS (4.2 K) | −1.54 | −1.53 ± 0.20 | −1.93 ± 0.26 | −2.13 ± 0.28 | (−)1.20 | −1.47 ± 0.20 | 1.84 ± 0.24 | −1.99 ± 0.26 | | −1.36 ± 0.18 | −1.68 ± 0.23 | −1.71 ± 0.24 |
| QS (77 K) | −1.18 | | | | (−)0.95 | | | | (−)0.82 | | | |
| IS (4.2 K) | 0.90 | | | | 0.92 | | | | | | | |
| IS (77 K) | 0.87 | | | | 0.85 | | | | 0.73 | | | |
| $\rho(0)$[c] | | 11 580.39 | 11 581.09 | | | 11 580.43 | 11 581.14 | | | 11 580.41 | 11 581.16 | |
| SOMO | | | | | | | | | | | | |
| % Fe | 75 | 13 | 11 | 10 | 63 | 58 | 46 | 46 | | 40 | 32 | 31 |
| % Cp | | 7 | 9 | 8 | | 25 | 36 | 37 | | 48 | 57 | 58 |
| % Bz | | 80 | 80 | 82 | 10−15[d] | 17 | 18 | 17 | 15−30[d] | 12 | 12 | 11 |
| Fe charge (AIM) | | 0.73 | 0.75 | | | 0.75 | 0.77 | | | 0.73 | 0.75 | |
| Fe spin (AIM) | | 1.02 | 1.16 | | | 1.03 | 1.18 | | | 1.03 | 1.20 | |
| Fe charge (NBO) | | 0.35 | 0.42 | 0.43 | | 0.38 | 0.44 | 0.46 | | 0.36 | 0.42 | 0.44 |
| Fe spin (NBO) | | 0.86 | 0.98 | 0.98 | | 0.87 | 1.01 | 1.01 | | 0.86 | 1.02 | 1.02 |
| Cp charge (NBO) | | −0.31 | −0.39 | −0.40 | | −0.27 | −0.35 | −0.36 | | −0.21 | −0.30 | −0.31 |
| Bz charge (NBO) | | −0.04 | −0.03 | −0.03 | | −0.11 | −0.09 | −0.10 | | −0.16 | −0.13 | −0.13 |
| Cp spin (NBO) | | 0.13 | 0.08 | 0.08 | | 0.14 | 0.08 | 0.08 | | 0.14 | 0.08 | 0.08 |
| Bz spin (NBO) | | 0.01 | −0.06 | −0.06 | | 0.00 | −0.09 | −0.09 | | −0.01 | −0.10 | −0.10 |

[a] Reference 5. The sign of the quadrupole splitting for CpFe($\eta^6$-$C_6Me_6$) was determined to be negative in later Mössbauer experiments,[37,41] and it is assumed to be negative for CpFe($\eta^6$-$C_6H_6$) and ($C_5Me_5$)Fe($\eta^6$-$C_6H_6$) as well. [b] $\eta$ is the asymmetry parameter, defined as $(V_{xx} - V_{yy})/V_{zz}$. [c] $\rho(0)$ is the calculated contact charge density at the iron nucleus. [d] Reference 10. Estimated from reduction potentials using the Vlcek method.

Downloaded by CARLI CONSORTIUM on June 29, 2009
Published on February 24, 2000 on http://pubs.acs.org | doi: 10.1021/om000034f

calculated quadrupole splittings than P86. That the hybrid functionals yield larger quadrupole splittings than BP86 is expected because of the dependence of $V_{zz}$ on $\langle r^{-3}\rangle$, where $r$ is the electron position coordinate.[42] The inclusion of Hartree−Fock exchange tends to contract the charge density around each atomic nucleus. This leads to shortened bond lengths (Table 1), larger atomic charges (Table 2), and larger values of $\langle r^{-3}\rangle$, which in turn increases $V_{zz}$ and the quadrupole splitting in accordance with eq 1. The asymmetry parameter, $\eta$, is small in all cases, increasing the quadrupole splitting by less than 2%. (The theoretical maximum increase, when $\eta = 1$, is 15.5%.) These asymmetry parameters are much less than the value of 0.9 based on an Xα treatment of CpFe($\eta^6$-$C_6H_6$)[9] and are closer to the value of ∼0 based on fits of the Mössbauer spectra.[37]

The Mössbauer isomer shift is proportional to the contact charge density at the iron nucleus.[42] To calculate this quantity, it is necessary to know the charge density at the iron nucleus in the molecule of interest and in the reference material. Because the latter quantity is constant, it is sufficient to show that calculated changes in contact charge density correlate linearly with experimentally measured isomer shifts across a series of compounds. The observed isomer shifts for six different compounds of the form ($C_5R_5$)Fe($C_6R'_6$) were found to be in the range 0.73−0.74 mm/s at room temperature and 0.81−0.87 mm/s at 77 K.[5,41] Four of these compounds, CpFe($\eta^6$-$C_6Me_6$), CpFe($\eta^6$-$C_6Et_6$), ($C_5Me_5$)Fe($\eta^6$-$C_6Me_6$), and CpFe($\eta^6$-$C_6H_6$), were also examined at 4.2 K and had isomer shifts of 0.90−0.92 mm/s. At a given temperature, these compounds all have nearly identical isomer shifts (the experimental error was 0.01 mm/s based on the statistical error in data fitting),[5] and the isomer shift clearly increases with decreasing temperature. ($C_5Me_5$)Fe($\eta^6$-$C_6H_6$) was anomalous in that its isomer shift of 0.73 mm/s at 77 K was much lower than that of the other complexes. With only this one measured value, it is impossible to say whether its isomer shift at 4.2 K would be about 0.9 mm/s, as with the other complexes, or again anomalously low. At 77 K the isomer shifts decrease from CpFe($\eta^6$-$C_6Me_6$) to CpFe($\eta^6$-$C_6H_6$) to ($C_5Me_5$)Fe($\eta^6$-$C_6H_6$), paralleling the trend in quadrupole splitting. At 4.2 K a trend is not obvious because there is no experimental value for ($C_5Me_5$)Fe($\eta^6$-$C_6H_6$) and the values for CpFe($\eta^6$-$C_6Me_6$) and CpFe($\eta^6$-$C_6H_6$) are very close (0.90 and 0.92 mm/s, respectively). This small increase is consistent with the DFT calculations[43] (Table 2) using either BP86 or B3P86. However, these two functionals give different predictions about the isomer shift for ($C_5Me_5$)Fe($\eta^6$-$C_6H_6$). BP86 predicts that its isomer shift should be between

(42) Goldanskii, V. I.; Makarov, E. F. In *Chemical Applications of Mössbauer Spectroscopy*; Goldanskii, V. I., Herber, R. H., Eds.; Academic: New York, 1968; pp 1−113.

(43) Calculation of contact charge densities using Gaussian 98 required a small modification to Link 601 so that the Fermi contact integrals were contracted with the charge density rather than the spin density.

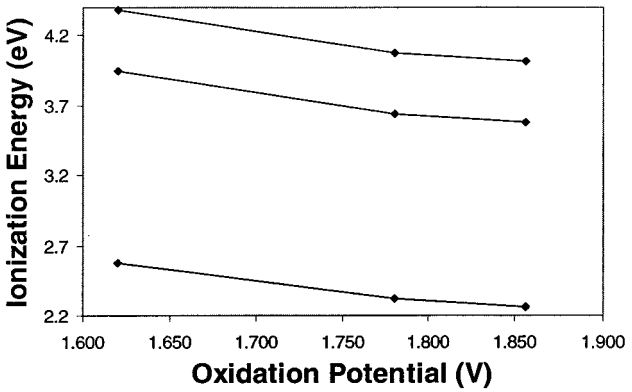


**Figure 1.** Calculated vertical ionization potentials plotted versus observed oxidation potential for (left to right) CpFe($\eta^6$-$C_6H_6$), CpFe($\eta^6$-$C_6Me_6$), and ($C_5Me_5$)Fe($\eta^6$-$C_6H_6$) using the (top to bottom) B3P86, B3LYP, and BP86 density functionals.

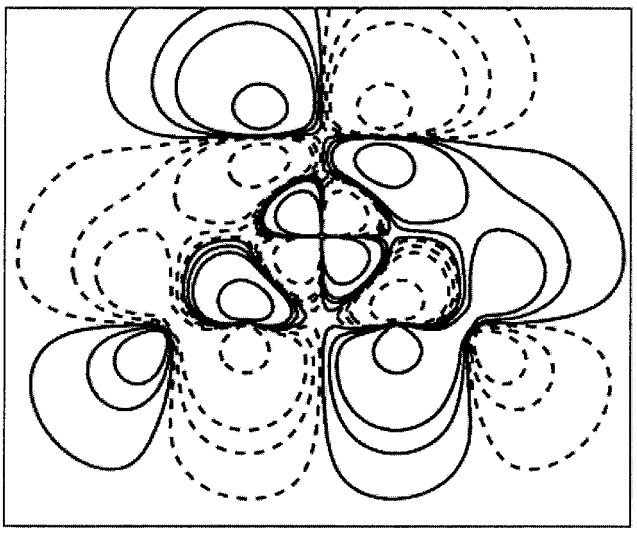

**Figure 2.** Contour plot of the SOMO for CpFe($\eta^6$-$C_6Me_6$) calculated using the B3P86 density functional. Contour values are ±0.0001, 0.005, 0.001, and 0.01. The *yz* plane is shown, where the *z* axis is normal to the rings (the Cp ring is on top) and the plane passes through two ring carbons and two methyl carbons of the arene ring.

that of CpFe($\eta^6$-$C_6Me_6$) and CpFe($\eta^6$-$C_6H_6$), while B3P86 predicts that its isomer shift should be higher.

**Ionization Energies.** Electrochemical experiments carried out by Astruc et al. showed that the oxidation potential for the three molecules studied here increased in the order ($C_5Me_5$)Fe($\eta^6$-$C_6H_6$) < CpFe($\eta^6$-$C_6Me_6$) < CpFe($\eta^6$-$C_6H_6$). Oxidation potentials are related to ionization energies, and the latter may be obtained as the negative of the highest occupied DFT orbital energy.[44] The vertical ionization energies calculated using DFT for these molecules reproduce the experimental trend of oxidation potentials, as shown in Figure 1.

The calculated properties are in reasonable agreement with the experimental values for these molecules, and we now discuss their electronic structure.

**The SOMO.** Table 2 includes the calculated composition of the highest-energy singly occupied molecular orbital (SOMO) for each of the three molecules studied here, and a contour plot of the SOMO of CpFe($\eta^6$-$C_6Me_6$) is shown in Figure 2. Plots of the SOMO and LUMO for all three molecules clearly show a metal d orbital antibonding to one of the $E_{1g}$ orbitals of benzene and cyclopentadienide. In the case of CpFe($\eta^6$-$C_6H_6$) and ($C_5Me_5$)Fe($\eta^6$-$C_6H_6$) the SOMO has A′ symmetry and the iron d orbital is designated $d_{xz}$, but in the case of CpFe($\eta^6$-$C_6Me_6$) the SOMO has A″ symmetry and the iron orbital is $d_{yz}$.[45] Thus, permethylation of the benzene ring actually switches the frontier spin-up orbitals relative to CpFe($\eta^6$-$C_6H_6$).[46] Additionally, the SOMO of CpFe($\eta^6$-$C_6Me_6$) acquires much more benzene character than the LUMO of CpFe($\eta^6$-$C_6H_6$) and ($C_5Me_5$)Fe($\eta^6$-$C_6H_6$). This is due to a large contribution from the 2s orbitals of the carbon atoms in permethylbenzene ring. This is not evident from the SOMO plot in Figure 2 because the largest coefficients are actually on the most diffuse components of the 2s orbitals (recall that each orbital basis function is triple-ζ), and these components do not influence the shapes of the high-valued contours. Although the SOMO for all three molecules is antibonding between the π system of each ligand ring and the metal 3d orbital, in the case of CpFe($\eta^6$-$C_6Me_6$) the SOMO is bonding between the 2s orbitals of four of the ring carbons and the iron 3d orbital. Extended Hückel and Xα calculations performed on a series of CpFe(arene) compounds in which the arene increased in size from benzene to naphthalene to pyrene also predicted a large increase in arene character of the SOMO.[10] Electrochemical measurements on CpFe($\eta^6$-$C_6H_6$) and ($C_5Me_5$)-Fe($\eta^6$-$C_6H_6$) led to estimates of 10−15% and 15−30% arene contribution to the SOMO, respectively.[10,47] These estimates were based on the Vlcek equation, which has been shown to be generally unreliable for estimating orbital compositions,[48] and Astruc et al. pointed out that the half-wave potentials for the ligands in these complexes, which are required for use of the Vlcek equation, are not known.[5] That these estimates agree with the DFT results must therefore be regarded as a coincidence. In summary, the DFT results indicate that the effect of permethylation is different for the Cp ring and the benzene ring in these molecules.

**Charge and Spin Density.** Two further points of comparison for the three molecules examined here are the charge and the spin density on the iron atom. These two quantities are directly related to the Mössbauer and EPR parameters, respectively. They were calculated using both the natural bond orbital (NBO) method of Weinhold et al.[49] and the atoms-in-molecules (AIM) method[50] of Bader et al.[51,52] The AIM method is based

(44) Casida, M. E. *Phys. Rev. B* **1999**, *59*, 4694−4698.

(45) For all molecules, we designate the *xz* plane as the mirror plane of symmetry, with the *z* axis being essentially normal to both rings. Saillard et al. found an A′ SOMO by DFT for all three of these molecules.

(46) The wave function stability calculation on CpFe($\eta^6$-$C_6Me_6$) specifically checked that switching the occupancy of the A′ and A″ orbitals did not lower the energy. This supports the belief that the wave function is not that of an electronically excited state. For all three molecules the SOMO−LUMO gap in the spin-up manifold was calculated to be 0.5−0.6 eV using BP86 and 2.9−3.2 eV with the hybrid functionals. Increasing the size of the basis set on iron by decontracting the most diffuse s, p, and d functions did not lead to a different occupation of the frontier orbitals.

(47) Lacoste, M.; Astruc, D. *J. Chem. Soc., Chem. Commun.* **1987**, 667−669.

(48) Schut, D. M.; Keana, K. J.; Tyler, D. R.; Rieger, P. H. *J. Am. Chem. Soc.* **1995**, *117*, 8939−8946.

(49) Reed, A. E.; Curtiss, L. A.; Weinhold, F. *Chem. Rev.* **1988**, *88*, 899−926.

Downloaded by CARLI CONSORTIUM on June 29, 2009
Published on February 24, 2000 on http://pubs.acs.org | doi: 10.1021/om000034f

Downloaded by CARLI CONSORTIUM on June 29, 2009
Published on February 24, 2000 on http://pubs.acs.org | doi: 10.1021/om000034f

on integration of the electron density within atomic basins whose boundaries, termed zero-flux surfaces, are defined by the topology of the electron density itself. An important distinction between the AIM approach and orbital-based methods such as the Mulliken and NBO analyses is that the AIM method is based directly on the electron density, which is an observable molecular property, whereas the other methods are based on the orbitals, which are not observables.[53] The assignment of the integrated charge to a particular atom in a molecule is still, of course, arbitrary. Both methods of population analysis indicate that both the charge and spin density on the iron atom in all three molecules is quite constant (Table 2). The spin density on iron is very large, in some cases exceeding unity, which indicates that significant spin polarization of the inner shell iron orbitals is occurring. The constant charge and spin density around the iron atom in these molecules is in contrast to the variable amount of metal character in the SOMO. The reason is that partial atomic charge and spin depend on the molecular electron density, which is itself determined by all of the molecular orbitals, not just the SOMO. Thus, in these three 19-electron complexes the occupation of an orbital that has a certain amount of metal character also causes changes in the already occupied orbitals such that the electron density around the metal stays fairly constant. Also, a large coefficient on a diffuse atomic orbital increases the contribution of that atom to the SOMO, but a diffuse orbital tends to distribute electron density over many atoms in a molecule. This is apparent in the case of CpFe($\eta^6$-$C_6Me_6$), where the large coefficients of the carbon 2s orbitals in the arene ligand are on the most diffuse of the three basis functions comprising the 2s orbital. Permethylation of either ring does not appreciably change the charge or spin density associated with the iron atom. This contrasts with the expected increase in electron donor ability of a ring ligand upon permethylation, but a synergistic effect of metal backbonding may compensate for this, a possibility that has already been proposed for these molecules.[9]

## Conclusions

DFT calculations indicated that the SOMO of CpFe($\eta^6$-$C_6Me_6$), CpFe($\eta^6$-$C_6H_6$), and ($C_5Me_5$)Fe($\eta^6$-$C_6H_6$) may not have as high an iron component as was estimated from the magnitude of the nuclear quadrupole coupling. The latter estimation neglects the orbital relaxation that occurs when the SOMO is occupied. The metal component of the SOMO for CpFe($\eta^6$-$C_6H_6$) and ($C_5Me_5$)Fe($\eta^6$-$C_6H_6$) (40−60%) is appreciably higher than in the 19-electron adducts that we have studied (20−30%), but in CpFe($\eta^6$-$C_6Me_6$) it is very low (10%). The SOMO of metal sandwich complexes may show a larger amplitude on the metal than in 19-electron adducts, but this is evidently not consistent. More experimental and computational data on 19-electron sandwich compounds is needed before definitive conclusions can be made about whether their electronic structure is consistently different from that of 19-electron adducts. It is tempting to try to correlate the amount of metal character in the SOMO with the observed reactivity of the complex, but it is difficult to predict chemical reactivity from the ground-state electronic structure of an isolated molecule. It is true that CpFe($\eta^6$-$C_6Me_6$) was the only 19-electron complex in the CpFe(arene) series that could be isolated and crystallized and that it also has the least amount of metal character in the SOMO of the three molecules studied here. However, the reaction responsible for preventing isolation of the other CpFe(arene) compounds was their dimerization through the benzene rings, and that CpFe($\eta^6$-$C_6Me_6$) did not do so is explainable as being due to the steric hindrance of the methyl groups rather than to the low metal character in the SOMO. In contrast, we have found that cobaltocene has a high metal amplitude in the SOMO, about 50%, yet it is easily isolated and does not dimerize.[24]

The net spin density around the iron atom as determined by the AIM and NBO methods is very high (about 1.0 or higher) and constant in all three molecules, which indicates that appreciable spin polarization of the inner shell iron orbitals is taking place. The charge density around the iron is also constant, which is in contrast to the relatively low and variable amount of metal character in the SOMO. This is at least partly due to a compensating relaxation of the other molecular orbitals that takes place in response to occupation of the SOMO such that the spin and charge densities around the iron atom change negligibly. In the case of CpFe($\eta^6$-$C_6Me_6$) it is also partly due to the fact that most of the SOMO consists of the those 2s orbitals on the carbons of the arene ligand which are too diffuse to effectively localize charge on this ligand.

Although orbitals are not observables, they are of profound interest to chemists for understanding both chemical reactivity and molecular structure. Because molecular orbitals are usually constructed from linear combinations of atomic orbitals, it is natural to discuss molecular electronic structure in terms of atomic contributions. The contribution of an atomic orbital to a molecular orbital is often estimated from the decrease in magnitude of an experimentally measured quantity relative to that for the free atom. Here, for example, the amount of iron character in the SOMO was estimated from the difference in the nuclear quadrupole coupling between the 19-electron complex and the corresponding 18-electron complex, relative to the coupling expected for an electron in a 3d orbital of a free iron atom.[6] Estimating atomic contributions to molecular orbitals in this way neglects the relaxation of the orbitals due to the addition of the 19th electron, and it assumes that the reference quantity (for the free atom) is free from error. Observed molecular properties depend on all of the molecular orbitals. The highest occupied

(50) AIM quantities were calculated using the PROMEGA algorithm of the AIMPAC package (Biegler-Konig, F. W.; Bader, R. F. W.; Tang, T. H. *J. Comput. Chem.* **1982**, *3*, 317−328; available from http://www.chemistry.mcmaster.ca/aimpac) and the wave function information in the .wfn file output by Gaussian 98 ("output = wfn"). The .wfn file was modified so that it included either the α spin orbitals or the $\beta$ spin orbitals. PROMEGA then calculated the α and $\beta$ atomic charges for Fe separately. The total atomic charge was obtained by adding these quantities, and the spin density was obtained by subtraction. Because the PROMEGA algorithm is very slow and because AIMPAC calculates AIM properties for only one atom per run, we only calculated the charge and spin for the iron atom.

(51) Bader, R. F. W. *Atoms in Molecules: A Quantum Theory*; University of Oxford: Oxford, U.K., 1990.

(52) Bader, R. F. W. *Chem. Rev.* **1991**, *91*, 893−928.

(53) Bachrach, S. M. In *Reviews in Computational Chemistry*; Lipkowitz, K. B., Boyd, D. B., Eds.; VCH: New York, 1994; pp 171−228.

orbital may be the most significant contributor, but the influence of the remaining orbitals is often not negligible. Current computational methods such as DFT that go well beyond the approximations of Hückel theory do not neglect the effects of spin polarization or orbital relaxation in determining molecular orbital compositions and do not require atomic reference data. As the demand for accuracy in relating molecular properties to electronic structure increases, neglecting the aforementioned effects must eventually become unacceptable, and in this case computational methods such as DFT will be useful. As shown here and elsewhere,[12,13] DFT is a reliable method for calculating the properties of 19-electron organometallic complexes and, therefore, it is a useful guide to the interpretation of experimental data.

**Acknowledgment.** This work was supported by the National Science Foundation and by the National Computational Science Alliance under Grant No. CHE990027N and utilized the NCSA HP-Convex Exemplar SPP-2000. We are grateful to Prof. J.-Y. Saillard for communicating results prior to publication.

OM000034F

Downloaded by CARLI CONSORTIUM on June 29, 2009
Published on February 24, 2000 on http://pubs.acs.org | doi: 10.1021/om000034f